INTERNATIONAL JOURNAL FOR NUMERICAL METHODS IN FLUIDS
Int. J. Numer. Meth. Fluids 2000; **33**: 157–174

Dynamics of a small bubble in a compressible fluid

A. A. Aganin*

Institute of Mechanics, The Russian Academy of Siences, Lobachevsky Street, 2/31, Kazan 420111, Russian Federation

SUMMARY

An efficient (simplified) method for solving problems of spherically symmetric dynamics of a small gas bubble in a compressible fluid is proposed. The method is based on the joint use of the full problem statement (the gas dynamics equations for the gas and the fluid) and its relevant simplifications. Some approximate statements are discussed. In the proposed method, the rarefaction and compression of the gas during the slow motion of the bubble surface is assumed to be uniform over the bubble volume. At the same time the fluid in the thin zone adjacent to the bubble is considered to be slightly compressible. Otherwise the gas dynamics equations are used for the gas and the fluid. The dynamics of the fluid in the thick external zone are described by the linear acoustics only. The proposed simplified method and two others used in literature are estimated by comparison of their numerical results with those obtained in full statement. Copyright © 2000 John Wiley & Sons, Ltd.

KEY WORDS: bubble dynamics; gas–fluid interface; shocks

1. INTRODUCTION

Beginning with the work by Lord Rayleigh [1], who examined the action of cavitation on bodies in water, and up to the late 1980s, the theoretical investigation of dynamics of a small gas bubble in a fluid was mainly conducted using ordinary differential equations (ODEs) [1–5]. Equations of such kind are often referred to as the Rayleigh–Plesset (RP) equation. The solution to the RP equation can be easily determined numerically. The RP equation is derived assuming that rarefaction/compression of the gas in the bubble is uniform over the bubble volume, the fluid is incompressible or slightly compressible. A new model leading to the RP equation was recently put forward by Nigmatulin *et al.* [6]. One feature of this model is that the fluid is divided into two zones. In the near (adjacent to the bubble) zone measuring 1–10 bubble radii, the fluid is assumed to be incompressible. In the far zone, the assumptions of the linear acoustics are used. The near and far zones are matched asymptotically through the

* Correspondence to: Institute of Mechanics, The Russian Academy of Siences, Lobachevsky Street, 2/31, Kazan 420111, Russian Federation.

Received March 1999
Revised July 1999

intermediate infinity. Another feature of this model is that it takes into account not only waves diverging from the bubble but also those reflecting from the external surface of the fluid.

In the early 1990s, a single bubble sonoluminescence phenomenon was experimentally found [7], showing considerable promise for physics and chemistry [8]. In a typical experiment on sonoluminescence a spherical flask of a few centimeters in diameter is filled with a compressible fluid (for example, the degassed water). With the help of transducers on the flask surface, a standing ultrasound wave is created in the fluid so that a small (a few microns in diameter) gas bubble is levitated near the center of the flask. The bubble executes periodic oscillations with a flash of light each cycle. Within the majority of the period of the external excitation, the variation of the bubble radius predicted by the RP equation is in good agreement with experimental data [4]. Large deviation is observed only in the last stage of the bubble collapse, especially when the flash of light is emitted. In particular, the temperature level predicted by the RP equation is significantly lower than that estimated in experiments [9]. A theoretical explanation to this fact is that the light flashes are caused by shock waves arising in the bubble as a result of the fast (supersonic) motion of the bubble surface in the course of the bubble collapse [9].

Bubble dynamics simulation allowing for shocks in the gas was for the first time performed by Wu and Roberts [9] on the basis of gas dynamics equations for the gas in the bubble. Assumptions for the fluid were like those used in deriving the RP equation. A similar approach was also adopted later in other works [10,11]. Simulation with the gas dynamics equations for the fluid as well as the gas was presented by Moss *et al*. [12]. Such an approach is more natural since it allows for shocks in both media. It is much more time-consuming, however, as compared with that by Wu and Roberts [9] based on the use of gas dynamics equations for the gas only. Clearly, the approach by Wu and Roberts [9] needs more computer time than solution of the RP equation.

The main goal of this paper is to present a low-cost but sufficiently accurate method for solving problems of dynamics of a small gas bubble in a compressible fluid. In this method, the gas in the bubble is described by the gas dynamics equations or by analytical expressions obtained on the assumption that rarefaction/compression of the gas is uniform over the bubble volume. The analytical expressions for the gas are used when the gas particle velocity in the bubble is small. The fluid is divided into two zones. As for the gas in the bubble, the gas dynamics equations or analytical expressions are used in the near zone. The analytical expressions for the fluid are obtained on the assumption of its slight compressibility. They are used when the difference between the current and initial densities of the fluid is small. In the far zone the fluid is governed by the equations of linear acoustics only. This allows one to exclude the far zone from the direct consideration. Its influence is taken into account through the boundary conditions on the external surface of the near zone.

When computing bubble dynamics, the gas dynamics equations were solved numerically by the Lax–Friedrichs method [9], with the code DYNA2D [12], and by the Godunov method [10,11]. It should be noted that the accuracy of the numerical solution is to a great extent determined by numerical resolution of spherical shocks converging to the pole of the spherical co-ordinate system (the bubble center) and reflecting from it. For example [13], errors in computation of strong shocks diverging from the pole can be more than 1000 per cent.

2. PROBLEM STATEMENT

A spherical gas bubble of radius r_b oscillates in the center of a spherical volume of a fluid of radius R_F (Figure 1). The bubble is small in comparison with the fluid volume ($r_b/R_F \sim 10^{-3}$). The oscillations are excited by the pressure p_F on the external surface $r = R_F$, r being the distance from the bubble center. The pressure p_F varies harmonically

$$p_F(t) = p_F^0 - \Delta p_F \sin \omega t, \quad p_F^0 = p_F(0) \tag{1}$$

where Δp_F and ω are the oscillation amplitude and the frequency respectively, t is the time.

The gas and the fluid are governed by the gas dynamics equations

$$\frac{\partial}{\partial t}(\rho r^2) + \frac{\partial}{\partial r}(\rho r^2 u) = 0 \tag{2a}$$

$$\frac{\partial}{\partial t}(\rho r^2 u) + \frac{\partial}{\partial r}(p r^2 + \rho r^2 u^2) = 2rp \tag{2b}$$

$$\frac{\partial}{\partial t}(E r^2) + \frac{\partial}{\partial r}[r^2(p+E)u] = 0 \tag{2c}$$

along with the equation of state

$$p = p(\rho, i) \tag{2d}$$

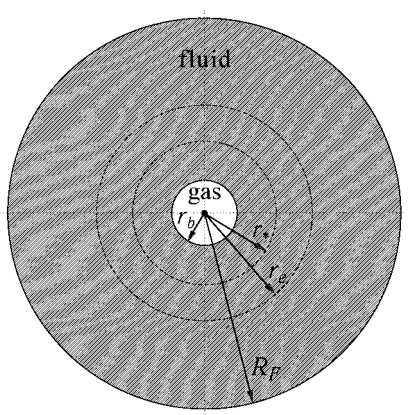

Figure 1. The gas bubble $0 \le r \le r_b$ and the near $r_b \le r \le r_*$, middle $r_* \le r \le r_e$ and far $r_e \le r \le R_F$ fluid zones.

Here u is the velocity, ρ is the density, E the specific total energy, p is the pressure, $i = E/\rho - u^2/2$ is the specific internal energy. The gas and the fluid are distinguished by the equation of state.

Boundary conditions on the surface $r = R_F$ and at the pole $r = 0$ are

$$p(R_F, t) = p_F(t), \qquad u(0, t) = 0 \tag{3}$$

Contact conditions on the bubble surface $r = r_b$ are

$$p(r - 0, t) = p(r + 0, t), \qquad u(r - 0, t) = u(r + 0, t) \tag{4}$$

When $t < 0$, the gas and the fluid are at rest. At $t = 0$

$$0 \le r \le r_b: \quad u = u^0 = 0, \quad p = p^0, \quad \rho = \rho_g^0 \tag{5a}$$

$$r_b \le r \le R_F: \quad u = u^0 = 0, \quad p = p^0, \quad \rho = \rho_f^0 \tag{5b}$$

From here on, the upper index 0 indicates the value of a parameter at $t = 0$, the lower indices g and f specify that a parameter corresponds to the gas and the fluid respectively.

The system (1)–(5) is below referred to as a full statement, although it does not take into account many physical aspects of the bubble dynamics under consideration. For example, it does not include the bubble surface tension, the heat conductivity and viscosity of the gas and the fluid, or the mass diffusion through the bubble surface. We shall also consider only the case of simple equations of state, which do not allow for vibrational degrees of freedom, dissociation and ionization taking place at high temperatures arising in the final stage of the bubble collapse. Inclusion of all these physical factors is not necessary for the purpose of the present work and will be published somewhere else. We just note here that it does not influence the main points of the proposed numerical method. Moreover, with increasing complexity of the statement they become more useful.

The solution to the system (1)–(5) is usually determined numerically, which is time consuming, however, because of the small ratio r_b/R_F. Time consumption can be reduced significantly if the full statement (1)–(5) is used along with one or the other of its relevant simplifications.

3. SOME APPROXIMATE STATEMENTS

3.1. Isentropic approximation

If there is no shock in both media, system (2) can be replaced by the following system:

$$\frac{\partial \rho}{\partial t} + u\frac{\partial \rho}{\partial r} + \rho\frac{\partial u}{\partial r} + \frac{2\rho u}{r} = 0, \qquad \frac{\partial u}{\partial t} + u\frac{\partial u}{\partial r} + \frac{1}{\rho}\frac{\partial p}{\partial r} = 0, \qquad p = p(\rho) \tag{6}$$

System (6) can be used only for one medium that does not have a shock.

3.2. Using fluid feature

When disturbances of the fluid are small then $(p-p^0)/p^0 \sim (10^3 \div 10^5)(\rho-\rho_f^0)/\rho_f^0$. Therefore, for the fluid disturbances up to tens of bars, one can write approximately instead of (6)

$$\frac{\partial \rho}{\partial t}+u\frac{\partial \rho}{\partial r}+\rho_f^0\frac{\partial u}{\partial r}+\frac{2\rho_f^0 u}{r}=0, \qquad \frac{\partial u}{\partial t}+u\frac{\partial u}{\partial r}+\frac{1}{\rho_f^0}\frac{\partial p}{\partial r}=0$$

$$p-p^0=(c_f^0)^2(\rho-\rho_f^0) \tag{7}$$

3.3. Acoustic approximation

If the excitation amplitude Δp_F is small, the convective terms in (7) at large distances from the bubble are small. Hence the equations of linear acoustics can be used. In acoustic approximation

$$\frac{1}{\rho_f^0}\frac{\partial \rho}{\partial t}+\frac{\partial u}{\partial r}+\frac{2u}{r}=0, \qquad \frac{\partial u}{\partial t}+\frac{1}{\rho_f^0}\frac{\partial p}{\partial r}=0, \qquad p-p^0=(c_f^0)^2(\rho-\rho_f^0) \tag{8}$$

where c_f^0 is the undisturbed speed of sound in the fluid.

3.4. Approximation of slightly compressible fluid

For a large radius of the fluid sphere R_F, in comparison with r_b, and for the wavelength of the external excitation $2\pi c_f^0/\omega$ of the order of R_F, significant displacements of the fluid in the near zone adjacent to the bubble take place together with small variations in density. Therefore, for the near fluid zone, the first two terms in the first equation of (7) can be omitted. Then system (7) reduces to

$$\frac{\partial u}{\partial r}+\frac{2u}{r}=0, \qquad \frac{\partial u}{\partial t}+u\frac{\partial u}{\partial r}+\frac{1}{\rho_f^0}\frac{\partial p}{\partial r}=0, \qquad p-p^0=(c_f^0)^2(\rho-\rho_f^0) \tag{9}$$

3.5. Approximation of uniform rarefaction/compression of the gas in the bubble

When the gas particle velocity in the bubble is small, the pressure in the bubble becomes nearly uniform. Then, system (6) reduces to

$$\frac{\partial \rho}{\partial t}+u\frac{\partial \rho}{\partial r}+\rho\frac{\partial u}{\partial r}+\frac{2\rho u}{r}=0, \qquad \frac{\partial p}{\partial r}=0, \qquad p=p(\rho) \tag{10}$$

4. SOME WAYS OF USING APPROXIMATE STATEMENTS

Let the interval $0 \le r \le R_F$ be divided into four portions (Figure 1): the area of the bubble $0 \le r \le r_b$ with the approximation of uniform rarefaction/compression (10), the near fluid zone $r_b \le r \le r_*^0$ (thin relative to R_F, $r_*^0/R_F \ll 1$) with the approximation of slightly compressible fluid (9), the middle $r_*^0 \le r \le r_e^0$ (also thin relative to R_F, $r_e^0/R_F \ll 1$) and the far $r_e^0 \le r \le R_F$ fluid zones with the acoustic approximation (8). The boundary conditions (4) are used on the surfaces $r = r_*^0$, $r = r_e^0$.

4.1. The area of the bubble

It follows from (10) that in the area of the bubble $0 \le r \le r_b$

$$\rho(r, t) = \rho_g^0 \left(\frac{r_b^0}{r_b}\right)^3, \qquad p(r, t) = p(\rho), \qquad u(r, t) = r\frac{u_b}{r_b} \tag{11}$$

where $u_b = u_b(t)$ is the bubble surface velocity.

4.2. The far fluid zone [6]

For the approximation of linear acoustics (8)

$$p = p^0 - \rho_f^0 \frac{\partial \varphi}{\partial t}, \qquad u = \frac{\partial \varphi}{\partial r}, \qquad \rho = \rho_f^0 + \frac{(p - p^0)}{(c_f^0)^2}$$

where φ is the potential of the form

$$\varphi = \frac{1}{r}\left[\psi_1\left(t - \frac{r}{c_f^0}\right) + \psi_2\left(t + \frac{r}{c_f^0}\right)\right]$$

At the boundary $r = r_e^0$

$$Q_e(t) = -\left[\psi_1\left(t - \frac{r_e^0}{c_f^0}\right) + \psi_2\left(t + \frac{r_e^0}{c_f^0}\right)\right] + \frac{r_e^0}{c_f^0}\left[-\psi_1'\left(t - \frac{r_e^0}{c_f^0}\right) + \psi_2'\left(t + \frac{r_e^0}{c_f^0}\right)\right]$$

where $Q_e(t) = (r_e^0)^2 u(r_e^0, t)$, the prime denotes the derivative with respect to the argument in brackets.

Since $r_e^0/R_F \ll 1$ then $r_e^0/c_f^0 \ll R_F/c_f^0$. Expanding functions

$$\psi_1\left(t - \frac{r_e^0}{c_f^0}\right), \quad \psi_1'\left(t - \frac{r_e^0}{c_f^0}\right), \quad \psi_2\left(t + \frac{r_e^0}{c_f^0}\right), \quad \psi_2'\left(t + \frac{r_e^0}{c_f^0}\right)$$

in Taylor series at the point t and omitting members of the order $(r_e^0/c_f^0)^2$ and higher, we obtain

$$Q_e(t) = -\psi_1(t) - \psi_2(t) \tag{12}$$

Using (12), we find

$$p(r_e^0, t) = p^0 - \frac{\rho_f^0}{r_e^0}\left[\psi_2'\left(t + \frac{r_e^0}{c_f^0}\right) - \psi_2'\left(t - \frac{r_e^0}{c_f^0}\right) - Q_e'\left(t - \frac{r_e^0}{c_f^0}\right)\right]$$

Again, expanding in series and dropping members of the order $(r_e^0/c_f^0)^2$ and higher, we obtain

$$p(r_e^0, t) = p^0 - \frac{\rho_f^0}{c_f^0}[2\psi_2''(t) + Q_e''(t)] + \rho_f^0 \frac{Q_e'(t)}{r_e^0} \tag{13}$$

The function $\psi_2''(t)$ is determined from the boundary condition on the external surface $r = R_F$. Using (12), we find

$$p_F(t) = p^0 - \frac{\rho_f^0}{R_F}\left[\psi_2'\left(t + \frac{R_F}{c_f^0}\right) - \psi_2'\left(t - \frac{R_F}{c_f^0}\right) - Q_e'\left(t - \frac{R_F}{c_f^0}\right)\right]$$

whence

$$\psi_2''(t) = \psi_2''\left(t - \frac{2R_F}{c_f^0}\right) - \frac{R_F}{\rho_f^0} p_F'\left(t - \frac{R_F}{c_f^0}\right) + Q_e''\left(t - \frac{2R_F}{c_f^0}\right) \tag{14}$$

Expressions (13) and (14) can be rewritten in the form

$$-\frac{1}{c_f^0} Q_e''(t) + \frac{1}{r_e^0} Q_e'(t) - \frac{p(r_e^0, t) - p_{ef}(t)}{\rho_f^0} = 0 \tag{15}$$

$$p_{ef}(t) = p_{ef}\left(t - \frac{2R_F}{c_f^0}\right) + \frac{2R_F}{c_f^0} p_F'\left(t - \frac{R_F}{c_f^0}\right) - \frac{2\rho_f^0}{c_f^0} Q_e''\left(t - \frac{2R_F}{c_f^0}\right) \tag{16}$$

where $p_{ef} = p^0 - (2\rho_f^0/c_f^0)\psi_2''(t)$. Physically p_{ef} would be the pressure in the center of the flask if there was no bubble in the fluid.

4.3. The middle zone

Expressions for the middle zone $r_*^0 \le r \le r_e^0$ similar to (12) and (13) are

$$Q_{*e}(t) = r^2 u, \qquad Q_{*e}(t) = -\psi_1(t) - \psi_2(t), \qquad p = p^0 - \frac{\rho_f^0}{c_f^0}[2\psi_2''(t) + Q_{*e}''(t)] + \rho_f^0 \frac{Q_{*e}'(t)}{r}$$

It follows from these expressions and boundary conditions for the middle zone that

$$\left(\frac{1}{r_*^0} - \frac{1}{r_e^0}\right) Q_{*e}' - \frac{p(r_*^0, t) - p(r_e^0, t)}{\rho_f^0} = 0 \tag{17}$$

The solution inside the middle zone is

$$u=\frac{Q_{*\mathrm{e}}}{r^2}, \qquad p=p(r_*^0,\,t)+\left(\frac{1}{r}-\frac{1}{r_\mathrm{e}^0}\right)\rho_\mathrm{f}^0 Q'_{*\mathrm{e}}, \qquad \rho=\rho_\mathrm{f}^0+\frac{p-p^0}{(c_\mathrm{f}^0)^2} \tag{18}$$

4.4. The near zone

If the approximation of slightly compressible fluid (9) is used for the near zone then

$$r^2u=Q_{\mathrm{b}*}(t), \qquad -\frac{Q'_{\mathrm{b}*}}{r}+\frac{Q_{\mathrm{b}*}^2}{2r^4}+\frac{p}{\rho_\mathrm{f}^0}=F(t)$$

It follows from these expressions and boundary conditions for the near zone that

$$\left(\frac{1}{r_\mathrm{b}}-\frac{1}{r_*^0}\right)Q'_{\mathrm{b}*}-\frac{1}{2}\left(\frac{1}{r_\mathrm{b}^4}-\frac{1}{(r_*^0)^4}\right)Q_{\mathrm{b}*}^2-\frac{p_\mathrm{b}-p(r_*^0,\,t)}{\rho_\mathrm{f}^0}=0 \tag{19}$$

The solution inside the near zone is

$$u=\frac{Q_{\mathrm{b}*}}{r^2}, \qquad p=\rho_\mathrm{f}^0\left(F+\frac{Q'_{\mathrm{b}*}}{r}-\frac{Q_{\mathrm{b}*}^2}{2r^4}\right), \qquad \rho=\rho_\mathrm{f}^0+\frac{p-p^0}{(c_\mathrm{f}^0)^2} \tag{20}$$

4.5. Lagrangian boundaries between zones

Expressions (15)–(20) have been obtained for the fixed Eulerian boundaries between the near and middle $r=r_*^0$ and middle and far $r=r_\mathrm{e}^0$ fluid zones. Sometimes it is more convenient to have them moving together with the medium. Corresponding formulae are readily derived from expressions (15)–(20) by replacing $r_*^0\to r_*=r(r_*^0,\,t)$, $u(r_*^0,\,t)\to u_*=u(r_*,\,t)$, $p(r_*^0,\,t)\to p_*=p(r_*,\,t)$, $r_\mathrm{e}^0\to r_\mathrm{e}=r(r_\mathrm{e}^0,\,t)$, $u(r_\mathrm{e}^0,\,t)\to u_\mathrm{e}=u(r_\mathrm{e},\,t)$, $p(r_\mathrm{e}^0,\,t)\to p_\mathrm{e}=p(r_\mathrm{e},\,t)$.

4.6. Further simplifications

If an approximate description is used in several neighboring zones, the expressions obtained above can be further simplified. For example, if approximate statements are used in all fluid zones then $Q_{\mathrm{b}*}=Q_{*\mathrm{e}}=Q_\mathrm{e}=Q$. We find from (15), (17) and (19) that for Lagrangian boundaries

$$\frac{1}{c_\mathrm{f}^0}Q''-\frac{1}{r_\mathrm{b}}Q'+\frac{1}{2}\left(\frac{1}{r_\mathrm{b}^4}-\frac{1}{r_*^4}\right)Q^2+\frac{p_\mathrm{b}-p_\mathrm{ef}}{\rho_\mathrm{f}^0}=0$$

This expression can be reduced to the form more convenient for computation if its first term is small and $|u_\mathrm{b}/c_\mathrm{f}^0|\ll 1$. In such a case

$$-\frac{1}{r_\mathrm{b}}Q'+\frac{1}{2}\left(\frac{1}{r_\mathrm{b}^4}-\frac{1}{r_*^4}\right)Q^2+\frac{p_\mathrm{b}-p_\mathrm{ef}}{\rho_\mathrm{f}^0}+\frac{r_\mathrm{b}}{\rho_\mathrm{f}^0 c_\mathrm{f}^0}\frac{\mathrm{d}}{\mathrm{d}t}\,(p_\mathrm{b}-p_\mathrm{ef})=0 \tag{21}$$

Similarly, expression (15) is simplified to the form

$$-\frac{1}{r_e}Q'_e+\frac{p_e-p_{ef}}{\rho_f^0}+\frac{r_e}{\rho_f^0 c_f^0}\frac{d}{dt}(p_e-p_{ef})=0 \tag{22}$$

Remark

Expressions (17) and (18) for the middle fluid zone can be derived from expressions (19) and (20) for the near zone since the terms with u^2 are small in the middle zone. This allows one to use the approximation of slightly compressible fluid for the middle zone as well as for the near zone rather than to search for a value of r_* in the interval $r_b \le r \le r_e$ such that the approximation of the linear acoustics can be utilized in the area $r > r_*$. In this case, the exact position of the boundary $r = r_*$ becomes unimportant. Therefore, the near and middle zones can be united to produce one near zone $r_b \le r \le r_e$ with the approximation of slightly compressible fluid. Then expression (21) reduces to

$$-\frac{1}{r_b}Q'+\frac{u_b^2}{2}+\frac{p_b-p_{ef}}{\rho_f^0}+\frac{r_b}{\rho_f^0 c_f^0}\frac{d}{dt}(p_b-p_{ef})=0 \tag{23}$$

According to (19) and (20), the solution in the zone $r_b \le r \le r_e$ takes the form

$$u=\frac{Q}{r^2},\qquad p=p_b+\rho_f^0\left(\frac{1}{r}-\frac{1}{r_b}\right)Q'-\frac{\rho_f^0}{2}\left(\frac{1}{r^4}-\frac{1}{r_b^4}\right)Q^2,\qquad \rho=\rho_f^0+\frac{p-p^0}{(c_f^0)^2} \tag{24}$$

5. METHODS OF COMPUTATION

5.1. Complete method

The complete method is numerical integration of the problem in its full statement (1)–(5). System (2) is used for simulation of the gas and the fluid everywhere in space and in time. The solution to system (2) is determined by the numerical technique [11] based on the Godunov method [14].

5.2. Simplified method 1 (similar to that of Nigmatulin et al. [6])

In this method, rarefaction/compression of the gas in the bubble is assumed to be uniform over the bubble volume. The fluid in the thin near zone adjacent to the bubble is taken to be slightly compressible. In the external area assumptions of linear acoustics are used. Therefore, the solution in the bubble is determined by expression (11), and by expression (24) in the near zone of the fluid. The parameter Q is found from the Equation (23).

5.3. Simplified method 2 (similar to that of Wu and Roberts [9])

In this method, the gas in the bubble is described by expression (11) when the gas particle velocity is small. Otherwise, the full system (2) is used. The description of the fluid is exactly the same as that in the simplified method 1. Hence, sometimes Equation (23) is solved together with system (2), and sometimes Equation (23) is solved together with expression (11). The changeover from expression (11) to system (2) is effected by the following conditions:

$$u_b < 0, \qquad M_{gb} = \frac{|u_b|}{c(r_b - 0, t)} > M^*_{gb} \tag{25}$$

where M^*_{gb} is some small critical value. Expression (11) is used again when the conditions in (25) are violated along with fulfillment of the inequality

$$\frac{p_{0bmax} - p_{0bmin}}{p(r_b - 0, t)} < \varepsilon_{0b}$$

where ε_{0b} is some small number, $p_{0bmin} = \min_{0 \le r \le r_b} p(r, t)$, $p_{0bmax} = \max_{0 \le r \le r_b} p(r, t)$.

5.4. Simplified method 3 (present work)

In this method, the interval $0 \le r \le R_F$ is divided into three portions: the area of the bubble $0 \le r \le r_b$, the near $r_b \le r \le r_e$ and the far $r_e \le r \le R_F$ fluid zones. Depending on the solution, the gas in the bubble is governed by either system (2) or system (10), the fluid in the near zone by system (2) or system (9). For the far fluid zone only linear acoustics is used. This means that the far zone is excluded from the direct consideration. Its influence is taken into account through boundary condition (15). In the initial time interval, system (10) is used for the gas and system (9) for the fluid (in the near zone). Therefore, the solution is determined by expression (11) in the bubble and by expression (24) in the fluid. The parameter $Q = Q_{be} = Q_e$ is found from Equation (23) in which p_{ef} is defined by (16). The changeover to the full system (2) for simulation of the gas and the fluid is effected by condition (25).

Expression (11) for the gas and (24) for the fluid are used again when

$$u_b > 0, \qquad \frac{p(r_b + 0, t)}{p^0} < a^*_{be}$$

where a^*_{be} is some critical number such that $(a^*_{be})^{-1}$ is small.

6. NUMERICAL RESULTS

To estimate the simplified methods 1–3, the problem is considered with the following input data: $\Delta p_F = 0.25$ bar, $\omega = 2\pi$ (45 kHz), $\rho^0_g \approx 1.16$ kg m^{-3}, $T^0_g = 300$ K, $c^0_f = 1500$ m s^{-1}, $\rho^0_f = 1000$ kg m^{-3}, $R_F = 5$ cm, $r^0_b = 10$ μm, $p^0_F = p^0 = 1$ bar. Here, T^0_g is the gas temperature at $t = 0$. The equations of state are

$$p = (\gamma - 1)\rho i$$

with $\gamma = 1.4$ for the gas (air) and

$$p = (\Gamma - 1)\rho i + k_1^2(\rho - k_2)$$

with $\Gamma = 7.15$, $k_1 \approx c_f^0$, $k_2 \approx \rho_f^0$ for the fluid (water).

6.1. Complete method

The numerical solution by the complete method is found in the moving co-ordinates. The uniform moving grid of 200 cells is used in the bubble. In the fluid the grid step is increased geometrically in the direction of the external boundary $r = R_F$. At any moment in time the size of the cell adjacent to the bubble surface is a quarter of the cell size of the uniform grid in the bubble. The grid of 3840 cells is initially used in the fluid. At $t \approx (R_F - r_b^0)/c_f^0$, when disturbances from the external boundary reach the bubble surface, the conservative interpolation on the grid of 1920 cells is made. Further computation is performed on the grid of 200 cells in the bubble and 1920 cells in the fluid.

The results by the complete method are presented in Figures 2–4. Figure 2 shows the pressure p as a function of radius r for seven time moments $t_{1-7} \approx 33.3$, 36.1, 38.9, 41.6, 44.5, 46.7, 49.9 μs (the number of the curve corresponds to the number of the time moment). The curves of Figure 2 characterize the variation of the pressure in the fluid at large (relative to r_b) distances from the bubble. The moment $t_1 \approx (R_F - r_b^0)/c_f^0$ corresponds to the beginning of the interaction between the incident disturbances and the bubble surface, the intervals $t_{k+1} - t_k$ are approximately equal to $\frac{1}{8}$ of the period of external excitation. It follows from Figure 2 that the presence of the small bubble does not influence the pressure distribution in the fluid in the area

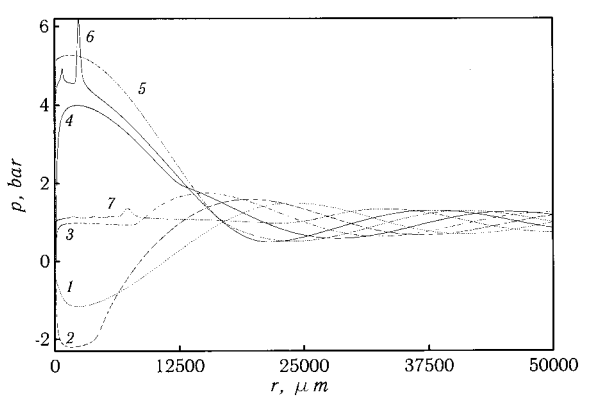

Figure 2. Distribution of the pressure p along the radius r at seven time moments $t_{1-7} \approx 33.3$, 36.1, 38.9, 41.6, 44.5, 46.7, 49.9 μs (the curve number corresponds to the number of the time moment) by the complete method.

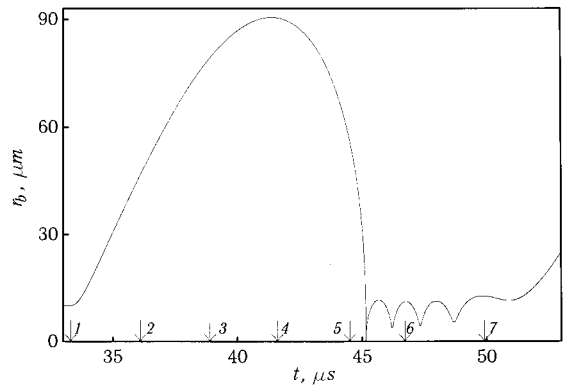

Figure 3. The bubble radius r_b as a function of time t by the complete method. The arrows indicate the time moments at which the curves are given in Figure 2 (the arrow number corresponds to the curve number).

$r > 2000$ μm. An exception is the short pulse in the interval $2000 < r < 4000$ μm in curve 6. At a later time this pulse is quickly dumped (curve 7).

Figure 3 shows the bubble radius r_b as a function of time t in the interval $33 < t < 53$ μs. The time moments for which the curves in Figure 2 are given are indicated in Figure 3 by arrows with corresponding numbers. According to the excitation (1) the bubble is first reached by the semi-wave with lower pressure (Figure 2, curve 1). Therefore, the bubble oscillations start with its expansion. In the course of the first oscillation, the bubble expands till $t = 41.6$ μs when $r_b = 90.56$ μm. At that moment, the pressure distribution in the fluid is close to that shown by curve 4 in Figure 2. The bubble next collapses, first slowly and then with greater speed. The

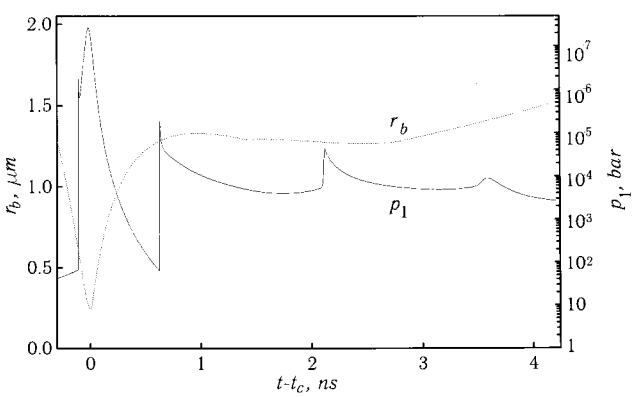

Figure 4. The bubble radius r_b and the pressure at the pole p_1 as functions of the relative time $t - t_c$ (t_c is the time at which the bubble radius takes its minimum value) by the complete method.

first oscillation of the bubble ends at $t = 41.15$ μs when $r_b = 0.245$ μm. After that, additional 3.5 oscillations of significantly less amplitude appear, then the next large oscillation begins.

Figure 4 shows the bubble radius r_b and the pressure at the pole p_1 as functions of the relative time $t - t_c$, where t_c is the time when the bubble radius takes its minimum value. The plot of the pressure p_1 has three jumps resulting from three shocks converging at the pole. The first jump is most intensive. After this jump the pressure grows up adiabatically by a factor of more than 10. The maximum value of the pressure p_1 is 27.3 Mbar. It is characteristic of the plot of the bubble radius r_b that in the interval $-0.3 < t - t_c < 0.3$ ns, the increase of r_b is almost as fast as the preceding decrease to the minimum value. Then, in the interval $0.6 < t - t_c < 3$ ns, the radius r_b remains nearly constant.

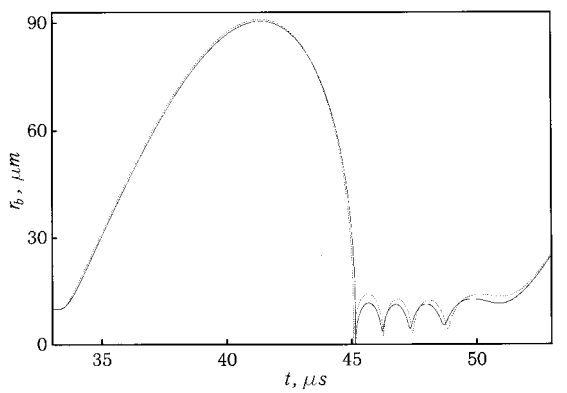

Figure 5. The bubble radius r_b as a function of time t by the simplified method 1 (· · ·) and the complete method (—).

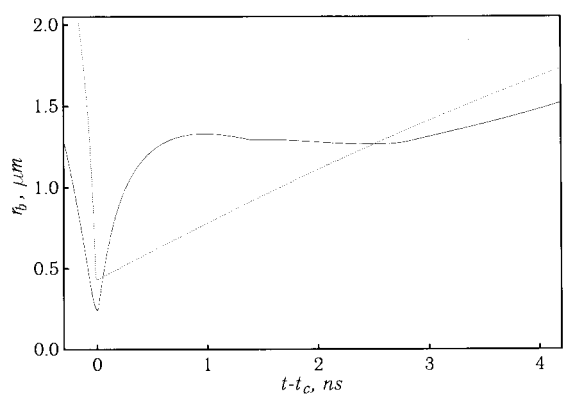

Figure 6. The bubble radius r_b as functions of the relative time $t - t_c$ by the simplified method 1 (· · ·) and the complete method (—).

6.2. Simplified method 1

Results by this method are presented in Figures 5–7 by the dashed curves. The solid curves given in those figures for comparison correspond to the complete method. Figure 5 shows the bubble radius r_b as a function of time t. One can conclude that the dashed and solid curves in this figure are in good agreement. More significant deviations are observed in Figures 6 and 7, where the bubble radius r_b (Figure 6) and the pressure at the pole p_1 (Figure 7) are shown as functions of the relative time $t - t_c$. In addition to the difference in the behavior of the curves due to, in particular, the assumption that there are no waves inside the bubble, the curves differ in their minimum values of r_b and maximum values of p_1. The simplified method

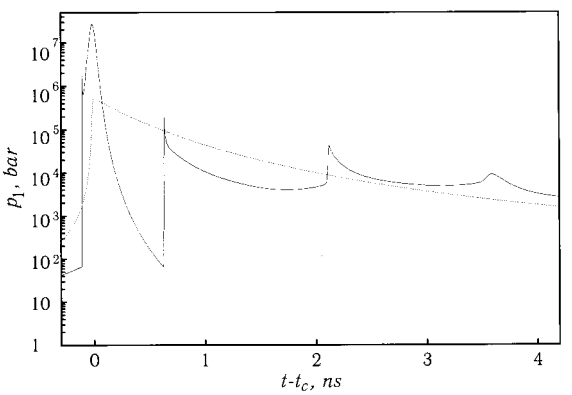

Figure 7. The pressure at the pole p_1 as functions of the relative time $t - t_c$ by the simplified method 1 ($\cdots$) and the complete method (—).

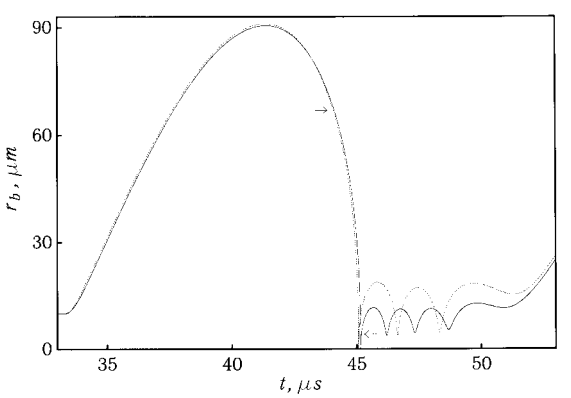

Figure 8. Same as in Figure 5 but by the simplified method 2 ($\cdots$) and the complete method (—).

1 gives the minimum value of r_b by 72 per cent greater, the maximum value of p_1 by two orders of magnitude less than those by complete method.

6.3. Simplified method 2

For the sake of comparison, the numerical solution to system (2) was obtained by this method using exactly the same (or very close to those) values of the grid parameters, which had been taken in computations by the complete method. In particular, the uniform moving grid of 200 cells was utilized. It was taken that $M^*_{gb} = 0.2$, $\varepsilon_{0b} = 0.05$. Results by the simplified method 2 (the dashed curves) in comparison with those by the complete method (the solid curves) are presented in Figures 8–10. Figures 8–10 are similar to Figures 5–7 except for the arrows in Figure 8 indicating the moments of the changeover from system (10) to system (2) (the upper

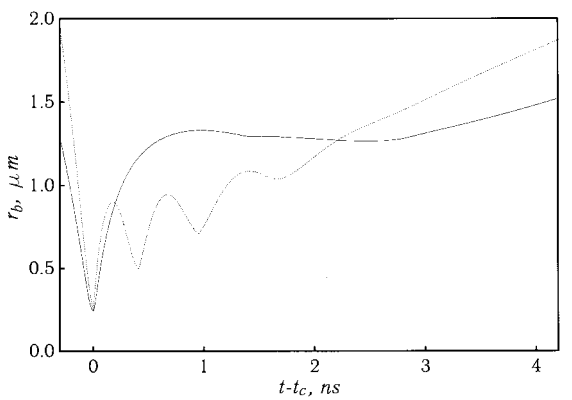

Figure 9. Same as in Figure 6 but by the simplified method 2 (· · ·) and the complete method (—).

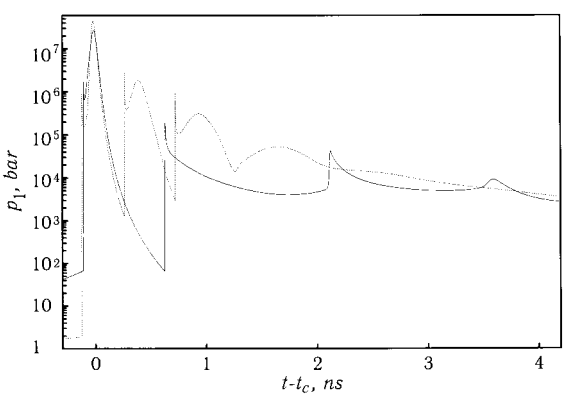

Figure 10. Same as in Figure 7 but by the simplified method 2 (· · ·) and the complete method (—).

arrow) and vice versa (the lower arrow) in the simulation of the gas in the bubble. In Figure 8, the most significant difference between the dashed and solid curves is observed after the first intensive collapse of the bubble. It is followed by the 2.5 small (relative to the first one) oscillations by the simplified method 2 rather than 3.5 by the complete method. The amplitude of those oscillations by the simplified method 2 is about twice as much as that by the complete method.

Generally, the difference between the dashed and solid curves in Figures 9 and 10, as in Figures 6 and 7, is large. Nevertheless, in Figure 9 the minimum values of the bubble radius r_b by the simplified and complete methods agree very well (up to 1 per cent). The agreement of maximum values of the pressure at the pole p_1 in Figure 10 is not so good. The maximum value of p_1 by the simplified method 2 is 45.2 Mbar, which is 66 per cent more than that by the complete method. The plots of p_1 by the simplified and complete methods have three jumps each. But the distance between the jumps along the axis $t - t_c$ in the solid curve is about twice as much as that in the dashed curve.

6.4. *Simplified method 3 (present work)*

Similar to the simplified method 2, the numerical solution to system (2) was obtained by the simplified method 3 using exactly the same (or very close to those) values of the grid parameters, which had been taken in computation by the complete method. In particular, the uniform moving grid of 200 cells was utilized in the area of the bubble. In the near fluid zone $r_b \le r \le r_e$, the grid step was increased geometrically in the direction of its external boundary $r = r_e$. At any moment in time, the size of the cell adjacent to the bubble surface was a quarter of the cell size of the uniform grid in the bubble. The number of the grid cells was 700. It was taken that $M^*_{gb} = 0.2$, $a^*_{be} = 300$.

The results by the simplified method 3 (the dashed curves) in comparison with those by the complete method (the solid curves) are presented in Figures 11–13, and are similar to Figures 8–10. Excellent quantitative agreement between the dashed and solid curves is observed in both figures. Qualitative agreement is also good enough. For example, the difference of the minimum

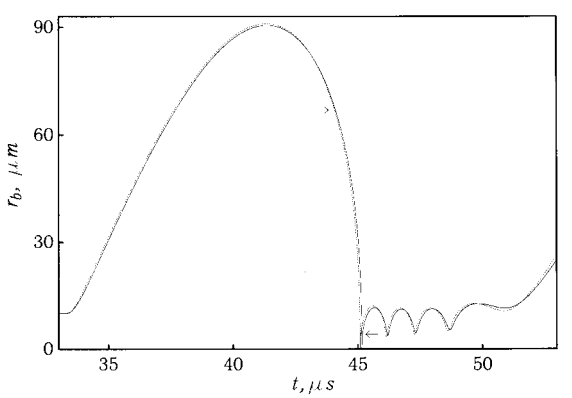

Figure 11. Same as in Figure 5 but by the simplified method 3 ($\cdots$) and the complete method (—).

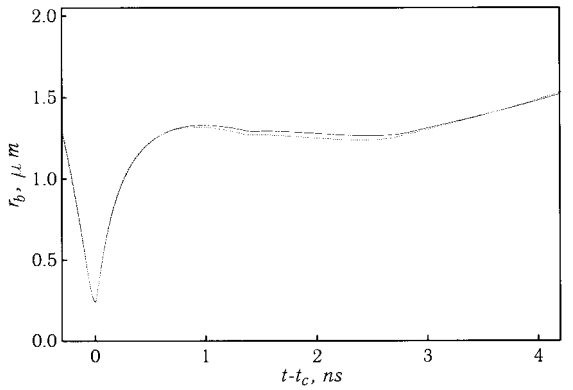

Figure 12. Same as in Figure 6 but by the simplified method 3 (· · ·) and the complete method (—).

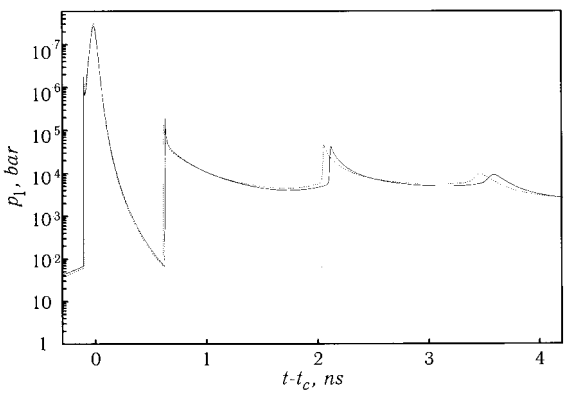

Figure 13. Same as in Figure 7 but by the simplified method 3 (· · ·) and the complete method (—).

values of the radius r_b (Figure 12) and the difference of the maximum values of the pressure at the pole p_1 (Figure 13) are less than 3 and 13 per cent respectively.

7. CONCLUSION

A low-cost but sufficiently accurate simplified method of solving problems of dynamics of a small gas bubble in a compressible fluid is proposed. The numerical results by this simplified method are found to be in good agreement with those by the complete method based on the full statement of the problem. A comparison of the numerical results by the complete method and simplified methods similar to those [6,9] used in literature is also performed. Their agreement in the final stage of the bubble collapse is shown to be significantly worse.

Low time consumption and high accuracy of the proposed method result from the joint use of the full statement (the gas dynamics equations for the gas and the fluid) and its possible simplifications (the uniform rarefaction and compression of the gas in the bubble; slight compressibility of the fluid in its thin zone adjacent to the bubble; linear acoustics in the far fluid zone).

The problem statement (1)–(5) does not include many physical aspects of the bubble dynamics (heat conductivity, viscosity, vibrational degrees of freedom, etc.), which are not necessary according to the objective of the present work. Clearly, the numerical solution taking them into account will require more computer time. In such a case, the proposed method correspondingly modified will be even more efficient and helpful.

ACKNOWLEDGMENTS

This work was supported by the Russian Foundation of Basic Research (project N 99-01-00234). The author is thankful to Professor M.A. Ilgamov for helpful discussions.

REFERENCES

1. Rayleigh Lord. On the pressure developed in a liquid on the collapse of a spherical cavity. *Philosophical Magazine* 1917; **34**: 94–97.
2. Plesset MS. The dynamics of cavitation bubbles. *Journal of Applied Mechanics* 1949; **16**: 277–282.
3. Nigmatulin RI. *Dynamics of Multiphase Media*, vol. 1. Hemisphere: Washington, DC, 1991.
4. Löfstedt R, Barber BP, Putterman SJ. Towards a hydrodynamic theory of sonoluminescence. *Physics of Fluids* 1993; **5**: 2911–2928.
5. Nigmatulin RI, Shagapov VSh, Vakhitova NK, Lahey RT Jr. A method for ultra high compression of gas bubbles in a liquid by the non-periodic vibrational action of pressure of moderate magnitude. *Physics–Doklady* 1995; **40**: 122–126 (translated from Russian).
6. Nigmatulin RI, Akhatov ISh, Vakhitova NK. The effect of fluid compressibility on the dynamics of the gas bubble. *Physics–Doklady* 1996; **41**: 276–279 (translated from Russian).
7. Gaitan DF, Crum LA, Roy RA, Church CC. Sonoluminescence and bubble dynamics for a single, stable cavitation bubble. *Journal of the Acoustics Society of America* 1992; **91**: 3166–3172.
8. Crum LA. Sonoluminescence, sonochemistry, and sonophysics. *Journal of the Acoustic Society of America* 1994; **95**: 559–562.
9. Wu CC, Roberts PH. Shock wave propagation in a sonoluminescencing gas bubble. *Physics Review Letters* 1993; **70**: 3424–3427.
10. Kondic L, Gersten JI, Yuan C. Theoretical studies of sonoluminescence radiation: radiative transfer and parametric dependence. *Physics Reviews E* 1995; **52**: 4976–4990.
11. Aganin AA, Ilgamov MA. Features of computation of the spherical waves by the Gudunov method. In *Simulation of Dynamics Processes in Continuous Media*. Izdatelstvo Kazanskogo matematicheskogo obchestva: Kazan, 1997; 108–193.
12. Moss WC, Clarke DB, White JW, Young DA. Hydrodynamic simulations of bubble collapse and picosecond somoluminescence. *Physics of Fluids* 1994; **6**: 2979–2985.
13. Noh WF. Errors for calculations of strong shocks using an artificial viscosity and an artificial heat flux. *Journal of Computers in Physics* 1978; **72**: 78–120.
14. Godunov SK (ed). *Numerical Solution of Multidimensional Problems in Gas Dynamics*. Nauka: Moscow, 1976.

